

Supplementary Information

Table of Contents

I.	Fabrication process of the microwall mixer.....	2
II.	Alternative electromagnetic setup for actuating the microwalls	4
III.	Mixing result using the electromagnetic setup	5
IV.	Measurement of the microwall speed using the electromagnetic setup.....	6
V.	Intensity of Segregation (IoS) method for quantification of mixing	8
VI.	Mixing with 3:1 flow rate ratio	9
VII.	Calculation of the pressure drop difference between 'on' and 'off' states.....	10
VIII.	COMSOL® Simulation setup.....	11
IX.	Other shapes created with FLAE/molding process	12

I. Fabrication process of the microwall mixer

In this section, we describe the fabrication process of our mixer in more detail. The process is based on replica micromoulding, and is modified from a previously reported one by us¹. The mould is fabricated from a 1 mm-thick fused silica wafer (SIEGERT WAFER GmbH, Germany) with a diameter of 100 mm and a surface roughness < 1 nm.

Using the FEMTOprinter f200 aHead (FEMTOprint SA, Switzerland) the fused silica wafer is exposed with a high-powered laser to locally modify the glass. The laser pulse energy and repetition rate used were 230 nJ and 1000 kHz, respectively. The laser was focused with a Thorlabs 20x microscope objective with a numerical aperture (NA) of 0.4. After a subsequent etching step in an ultrasonic bath with a concentrated solution of 45% potassium hydroxide (KOH, Sigma-Aldrich) diluted in water for approximately 7 hours, the desired negative shape of the structures in the glass mould is formed.

After etching, the mould received a silanization treatment with Trichloro(1H,1H,2H,2H-perfluorooctyl) silane, which turns the mould surface superhydrophobic and ensures that the moulding material, magnetic SIBS, will be easily released from the mould. Before the silanization process begins, the surface of the mould is activated using an oxygen plasma treatment carried out in a Plasma asher for 30 seconds and using a RF power of 20 Watts. After the surface activation, the dry silanization process begins by placing the mould in a vacuum chamber together with a vile filled with a small amount of the silane. The mould and silane are left under vacuum overnight during which the silane evaporates and is deposited onto the mould surface. After the silanization process is finished, the mould is thoroughly washed with IPA to remove the un-reacted silane.

The glass mould is then ready to be used in a hot embossing machine to create the active meandering structures from magnetic SIBS (poly(styrene-*block*-isobutylene-*block*-styrene). This magnetic SIBS is created by mixing SIBSTAR™ 073T (Kaneka Corporation) with carbonyl iron particles (BASF, average diameter 5 µm) in an extruder.

Once the materials and mould are ready, the magnetic SIBS can be formed into the desired shape using a hot embossing machine consisting of a manual press and heated plates (Specac Ltd Limited, England) see Figure A-1. Inside the hot embossing machine, the glass mould is placed between two brass plates to evenly transfer the heat from the machine to the material. To ensure the pressure is applied evenly throughout the mould, a 1 mm Teflon layer is placed into these brass plates together with a 0.505 mm silicon wafer for spacing. On top of the magnetic SIBS an additional 0.2 mm thick layer of Teflon is placed to ensure the polymer does not stick to the top brass plate.

The hot embossing process is performed by first heating the mould to 150 °C and maintaining this temperature for 5 minutes to ensure the entire polymer is heated. Once the polymer has reached the desired temperature, the pressure is increased to 5 tons and the mould is kept at this pressure and 150 °C for another 5 minutes to allow the magnetic SIBS to completely fill the cavities of the mould. After the magnetic SIBS is pressed into the desired shape, the mould is allowed to slowly cool down to 100 °C and the mould is removed from the hot embossing machine. The excess SIBS is removed by cutting away the material with a sharp knife approximately 2 mm away from the meandering structures; alternatively, the residual layer can also be completely removed using a 150 °C hot wire. When the excess material is removed, a 25 × 75 mm sheet of high impact polystyrene (HIPS) is placed over the magnetic SIBS structures in the mould, and the 1 mm-thick layer of Teflon is replaced by a 0.2 mm-thick layer. Thereafter, the hot embossing process is repeated once more, although this time the temperature is allowed to decrease until room temperature before releasing the pressure. Once the pressure is released, the mould is placed in an IPA bath for approximately 5 minutes to help lubricate the microwalls after which the HIPS sheet with microwalls can be released.

To attach the microwalls and HIPS sheet to the channel, a layer of 'Tesa 4965 Original' double-sided tape with a thickness of 205 μm is used. Using a CO₂ laser cutter, the tape is cut into shape after which it is placed onto the '3in1' microfluidic chip from ibidi®. Finally, the HIPS and microwalls are mounted in the device by aligning the microwalls to the channel under a microscope.

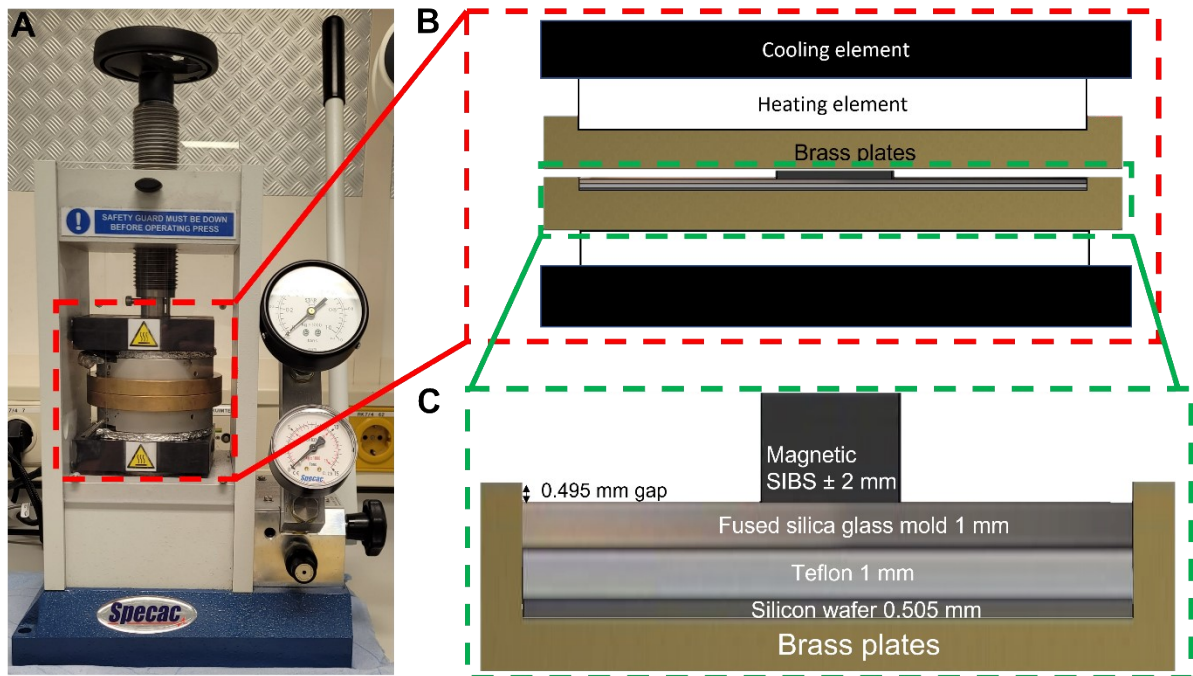


Figure A-1: A: Hot embossing machine from Specac Ltd Limited, England used for fabrication. B: Cut out section of the hot embossing machine showing the cooling and heating elements as well as the position of the brass plates (bronze), mould and magnetic SIBS (black). C detailed cross section showing how the mould is positioned inside the brass plates. For the second hot embossing step, the 1 mm Teflon layer is replaced by a 0.2 mm-thick layer of Teflon.

II. Alternative electromagnetic setup for actuating the microwalls

We have made a compact electromagnetic setup with only one pair of poles, which can also be used to actuate the microwalls to the 'on' position, see Figure A-2. However, this setup cannot be used to completely turn the microwalls to the 'off' position, because it cannot produce a horizontal magnetic field.

The core is made of laminated permalloy to reduce eddy current. The setup can generate a square wave magnetic field up to 150 mT at frequencies below 1 Hz. Above 1 Hz, the waveform starts to deviate from square shape due to inductance, see Figure A-2(C) versus (D).

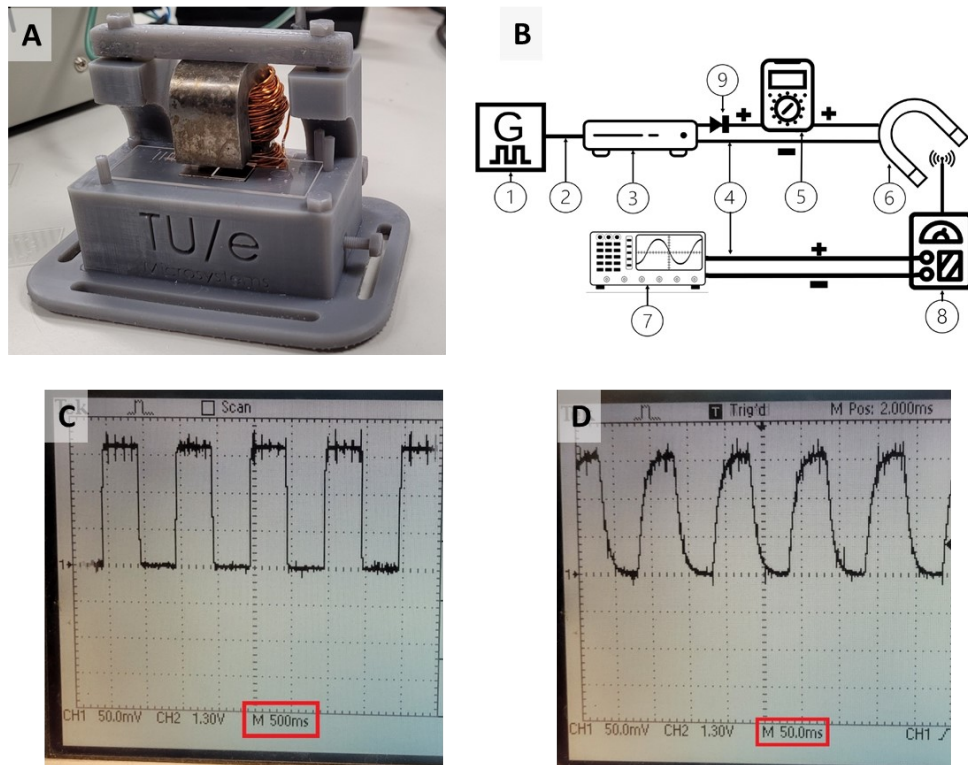


Figure A-2: In-house made electromagnetic setup as an alternative to the permanent magnet for actuating the microwalls to the 'on' position. (A) Picture of the setup. (B) Schematic view of the control and measurement of the setup: 1: Signal generator; 2: BCA to RCA coax cable; 3: Amplifier; 4: Banana plug cable; 5: Multimeter 6: Electromagnet; 7: Oscilloscope; 8: Gauss meter; 9: Diode. (C, D) Oscilloscope readout at 1 Hz and 10 Hz actuation frequencies. The measured amplitude is about 150 mT in both cases (1 mV corresponds to 1 mT).

III. Mixing result using the electromagnetic setup

We have also performed mixing experiments with the electromagnetic setup shown above. Since the magnetic field can only be turned on in the vertical direction, the microwalls cannot be fully collapsed into the 'off' state, so some level of mixing is always present.

Figure A-3 shows the mixing index achieved using the electromagnetic setup to actuate the microwalls. It can be seen that the relative change between on and off (or half off, compared to the fully collapsed state achieved by the permanent magnet) is less than shown in Fig 2 in the paper.

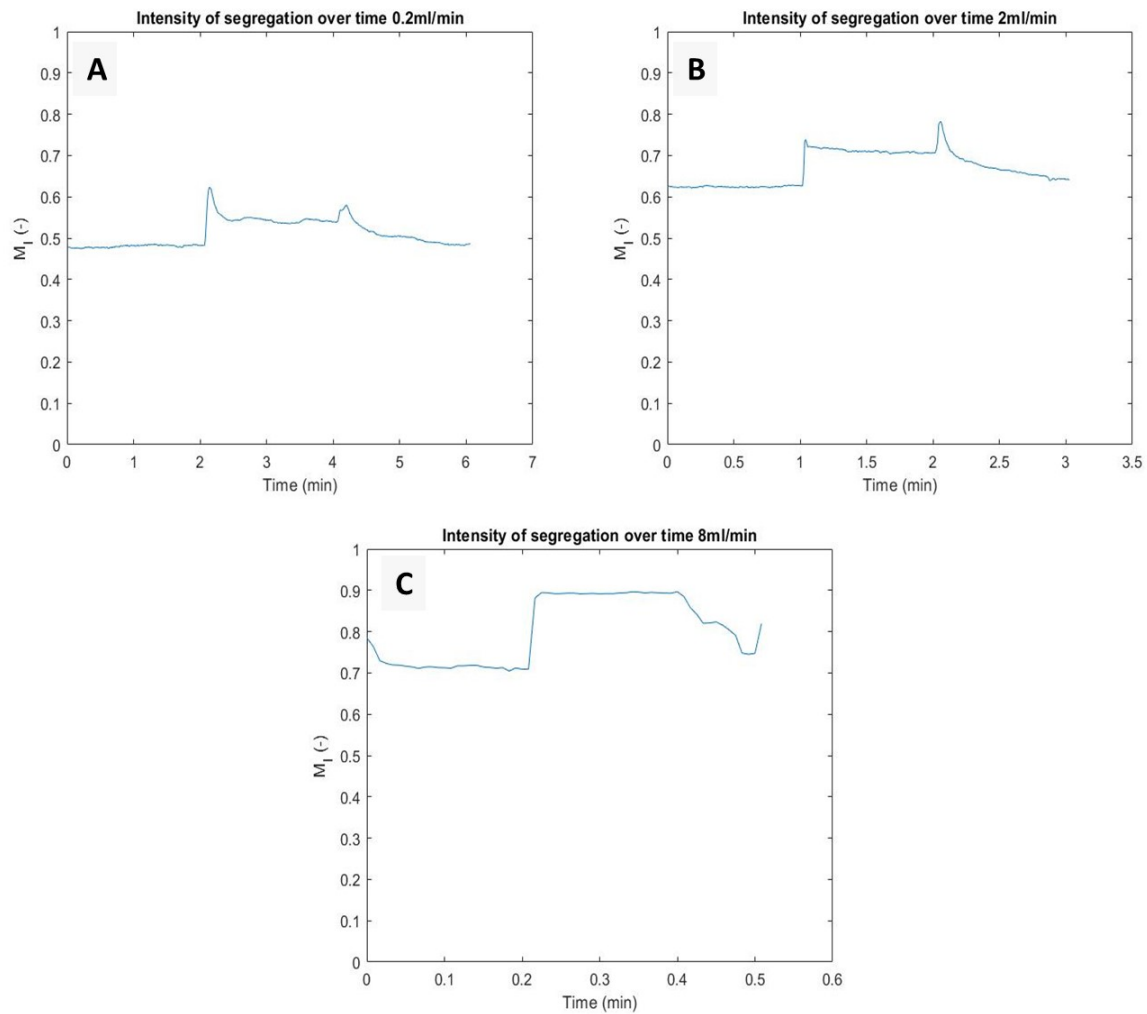


Figure A-3: Mixing Index measured under different flow rates in water, using the electromagnetic setup for actuation. The microwalls cannot be fully actuated into the 'off' state, so the differences in mixing index between 'on' and 'off' is not as large as when they are actuated with the permanent magnet, as shown in the main text of the paper. (A-C) mixing index over time at various flow rates, with the time of jump and drop in the index corresponding to the turning on and off of the electromagnet.

IV. Measurement of the microwall speed using the electromagnetic setup

We used the electromagnetic setup to measure the deflection of the microwalls from a side view. The initial angle and the thickness of the microwalls were varied, and the total deflection and the speed of the tip were measured at different actuation frequencies. A movie can be found in the supplementary information that shows the real-time tip movement and automatic tracking of the tip using MATLAB.

Figure A-4 shows the tip displacement and speed under various configurations. Overall, we can conclude that the speed of the microwalls is in the order of millimeters per second or faster, so the microwalls can be switched between 'on' and 'off' states in a fraction of a second, and for the application timescale (minutes) they can be seen as instantaneously switchable.

Note that these samples have a width (in-plane direction) of 1 mm and extended length about 350 μm (thin part length 255 μm). This is different from the microwalls in the main paper, which are 2.65 mm and 600 μm (extended length), respectively. The width should have minimum impact on the result, as both magnetic torque and bending stiffness scales linearly with the width. The length of the microwalls in the actual experiments is longer, and they have a higher aspect ratio, which is beneficial for magnetic actuation, since the magnetic moment increases with length and the bending stiffness is decreased.

Two different grades of SIBS were used to make the microwalls. Besides 073T, 062T was also tested, and they have different Young's Modulus (0.9 MPa and 0.7 MPa, respectively, from the company datasheet). Note that the results from this experiment are probably an underestimation of the actual reaction speed of the microwalls, as the magnetic field takes time to ramp up to the stable value from zero because of the inductance of the electromagnet. In the actual experiment, the microwalls are actuated with a permanent magnet, which also induces a slightly stronger magnetic field (surface magnetic flux density about 390 mT) than the electromagnet used here (maximum flux density 150 mT).

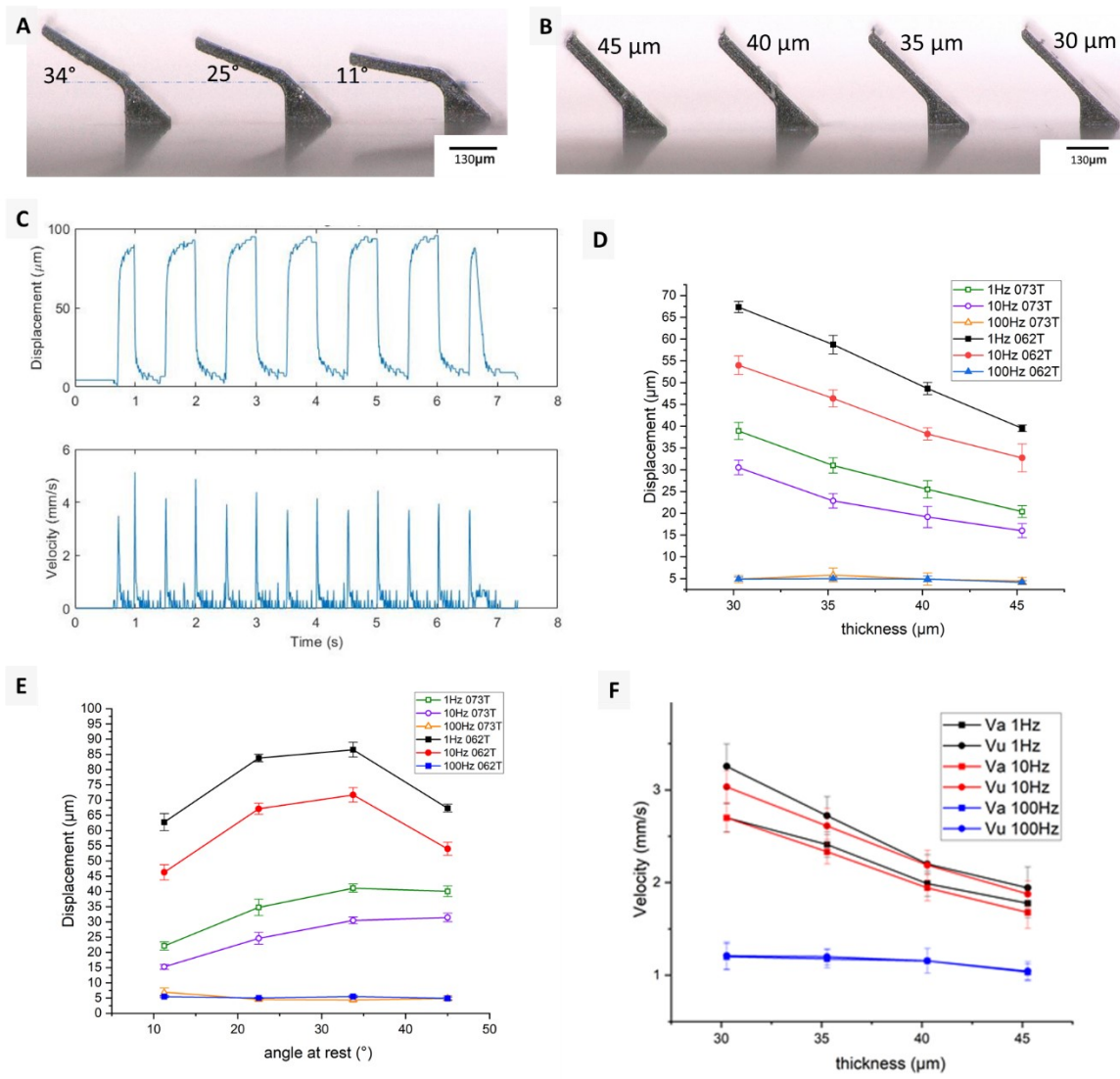


Figure A-4: Different microwall geometry and the measurement of deformation using the electromagnetic setup (side view). The top thin part is 255 μm long for all samples. (A) Samples with different resting angle, which are 34, 25 and 11 degrees, respectively. (B) Samples with different thicknesses, which are 45, 40, 35 and 30 μm , respectively. (C) Measured tip displacement and the tip velocity over time, at 1 Hz actuation frequency, for a sample having the thickness of 40 μm and resting angle of 45 degrees; matrix material is SIBS 073T. (D) Tip displacement with respect to the thickness for microwalls made with different matrix materials and at different actuation frequencies. (E) displacement with respect to rest angle. (F) tip velocity with respect to the microwall thickness. V_a is the speed of the tip moving up when the field is turned on, and V_u is the speed of the tip moving back when the field is turned off.

V. Intensity of Segregation (IoS) method for quantification of mixing

To use the IoS method for quantifying mixing using the images taken from the camera, we need to know the concentration of the dye with respect to the intensity values of the pixels, or to create a mapping between them. In our experiment, we use three data points to create this mapping: 0 %, 50 % and 100 %, which correspond to pure liquid, fully mixed, and pure dyed fluid, respectively. A second order polynomial fit was made to generate the complete curve between 0% and 100%.

Figure A-5 shows the second order polynomial mapping curve for water. For comparison, a simple linear mapping is also shown, and the calculated mixing indices using the two ways of mapping are shown in Figure A-5(B). It can be seen that, even though the mapping curves are significantly different, the resulting mixing indices both show a significant jump at the same time. The number is shifted upwards for polynomial mapping, both for mixed and unmixed fluids.

Another way to evaluate the two ways of mapping is to look at the average derived concentration of the frame of interest over time. In an ideal situation, the average concentration over the entire frame should keep at 0.5, or 50%. It can be seen from Figure A-5(C) that polynomial mapping generates a line that has less variation and closer to 50% over time. For those reasons, we chose polynomial fitting for processing the images.

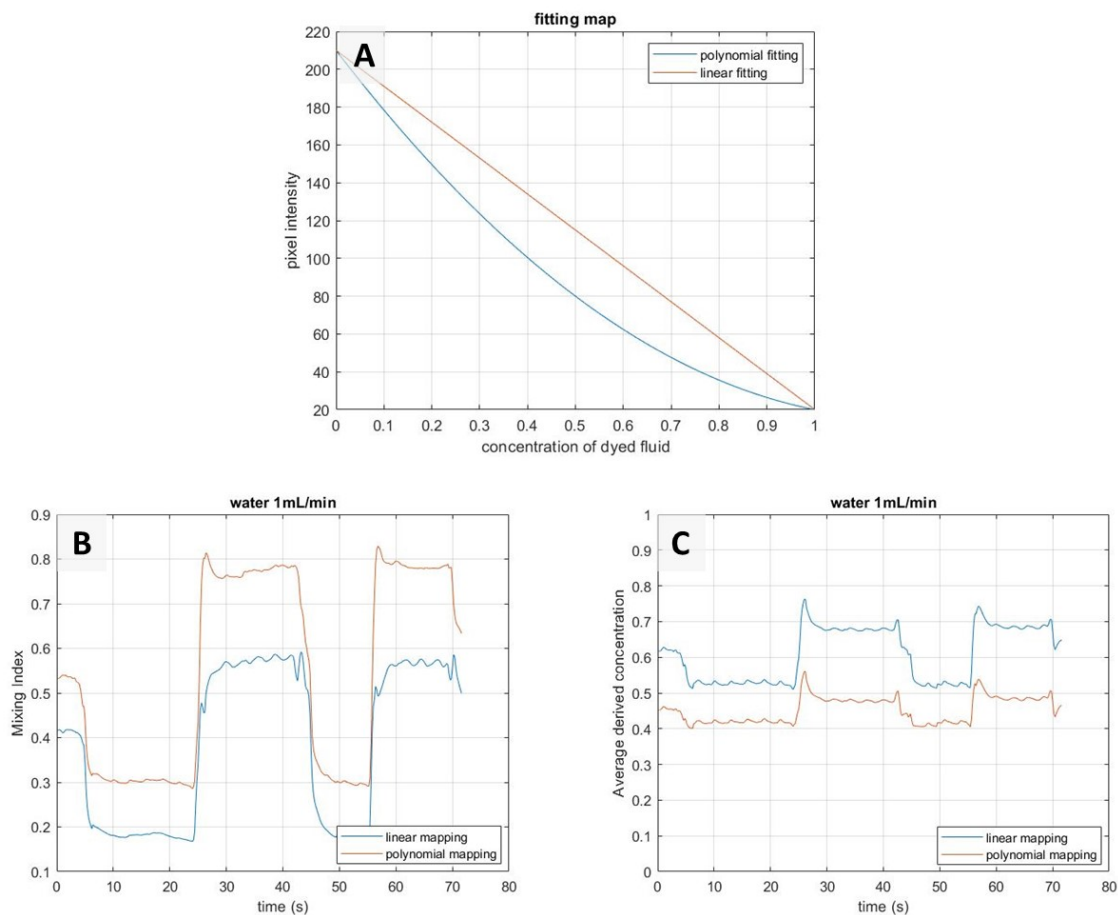


Figure A-5: Mapping of the pixel intensity to the concentration of dyed fluid for water. (A) Two different ways of mapping: 1. second order polynomial fit (blue) from three data points, namely the pixel intensities from 0 %, 50 % and 100 % dye concentrations; and 2, simple linear fit from 0% and 100% only. (B) Calculated mixing indices using the two different ways of mapping for 1 mL/min water. (C) Average concentration of each frame over time, calculated from different ways of mapping. Ideally the line should be as close to 0.5 as possible.

VI. Mixing with 3:1 flow rate ratio

The microwall mixer works for two streams with unequal flow rates as well. Figure A-6 shows the mixing results with 1:3 flow rate ratio of coloured vs clear water at different total flow rates.

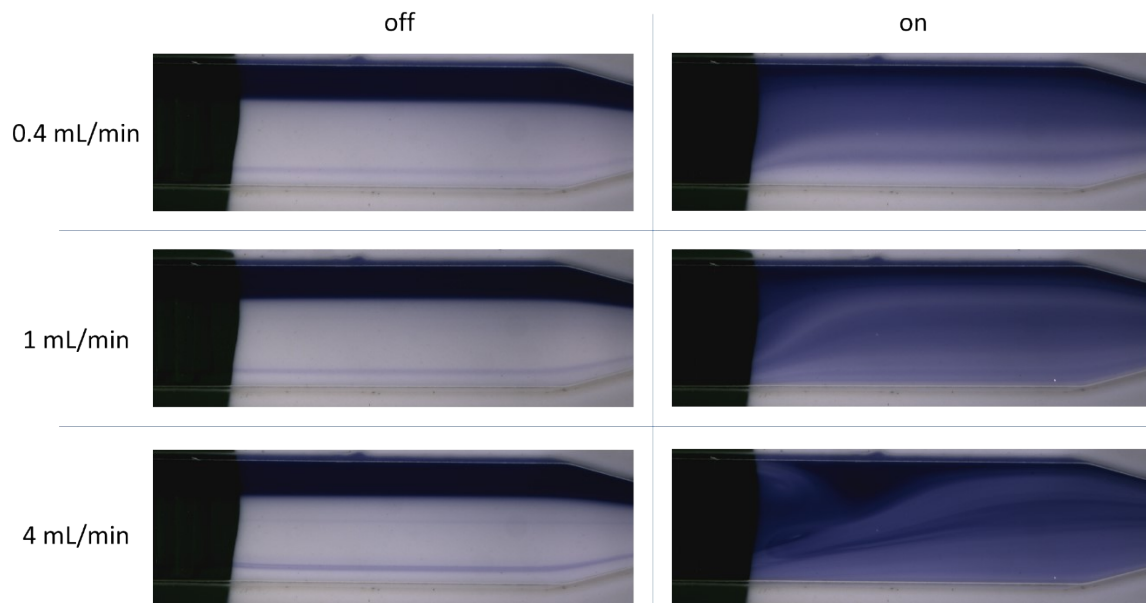


Figure A-6: Mixing results of two streams with unequal (1 to 3) flow rates. The text on the left shows the combined flow rates of the two streams.

VII. Calculation of the pressure drop difference between 'on' and 'off' states

If we assume a Poiseuille flow profile for both 'on' and 'off' states, the flow resistance can be calculated by the channel geometry²:

$$R = \frac{12\mu L}{wh^3 \left[1 - \frac{192h}{\pi^5 w} \sum_{i=1,3,5,\dots}^{\infty} \frac{\tanh(i\pi h/2w)}{i^5} \right]}$$

in which w is the channel width, h is the channel height and L is the channel length.

The exact analytical solution of R can also be approximated by:

$$R = \frac{12\mu L}{h^3 w [1 - 0.63(h/w)]}$$

For the specific configuration of the microwalls in the paper, when they are in the 'on' state, the total meandering path length is about 66 mm, the channel height is 0.6 mm and width is 0.45 mm, which gives $R_{on} = 5 \times 10^{10}$ Pa·s/m³ in water. In the 'off' state, the path length is returned to about 10 mm, the channel height remains almost unchanged, and the width returned to 3 mm, which gives $R_{off} = 2.1 \times 10^8$ Pa·s/m³. So the ratio of hydrodynamic resistance between 'on' and 'off' states are about 240 times in the section of the microwalls.

The pressure drop can then be calculated by:

$$\Delta P = RQ$$

in which Q is the flow rate. For 1 mL/min water flow, for example, the 'on' state will produce a 850 Pa pressure drop, compared with just 3.5 Pa for the 'off' state.

VIII. COMSOL® Simulation setup

The channel is 18 mm-long, 3 mm-wide and 0.6 mm-high. The microwalls are 2.65 mm-long, which leaves a 350 μm gap at the ends. Each microwall is 50 μm -thick and have a 500 μm pitch, which leaves 450 μm distance between walls. The microwalls are implemented as static boundaries with the same height as the channel (0.6 mm).

Water (1 mPa·s) is set as medium. Various flow rates are set as the boundary condition at the inlet, see Figure A-7, and the other end of the channel is set to be a free outlet (zero pressure). Incompressible, static flow with inertia is assumed:

$$\rho(\mathbf{v} \cdot \nabla)\mathbf{v} = \nabla \cdot -p\mathbf{I} + \boldsymbol{\tau}_v$$

where ρ is the density of water (1000 kg/m³), \mathbf{v} is the speed vector, p is the pressure, \mathbf{I} is the identity matrix, and $\boldsymbol{\tau}_v$ is the viscous stress tensor.

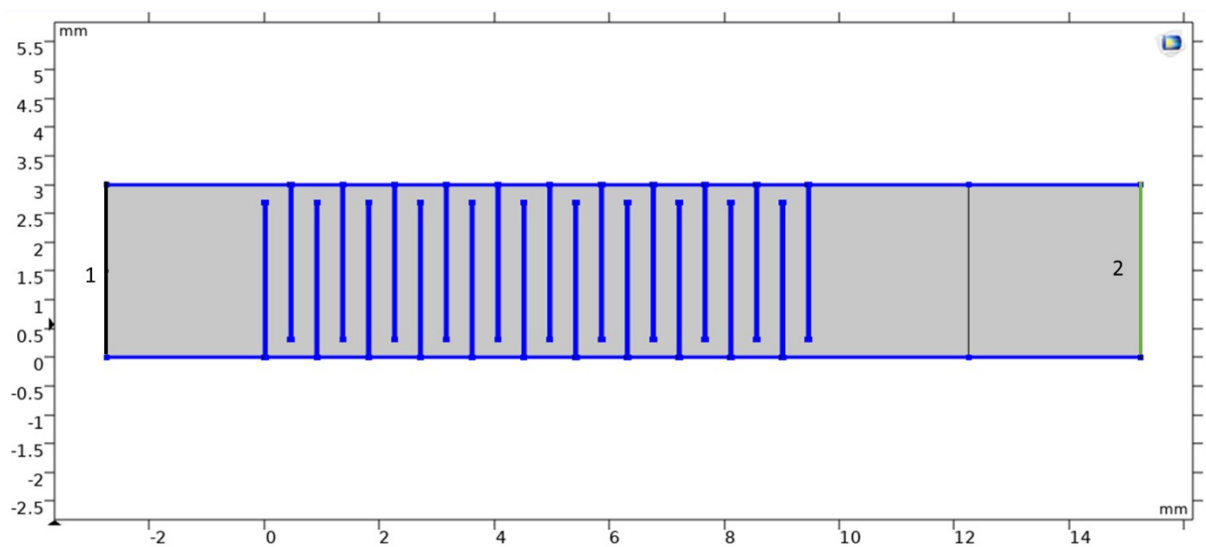


Figure A-7: Top view of the channel geometry used in COMSOL® simulation. Boundary 1 is set as flow inlet, and boundary 2 is set as free outlet.

IX. Other shapes created with FLAE/molding process

Besides the microwalls shown in the main text of the paper, we have also tested other shapes and configurations. These shapes are found to be not as effective for mixing compared to the microwalls (with the available actuators), but they showcase the flexibility of the FLAE/molding process.

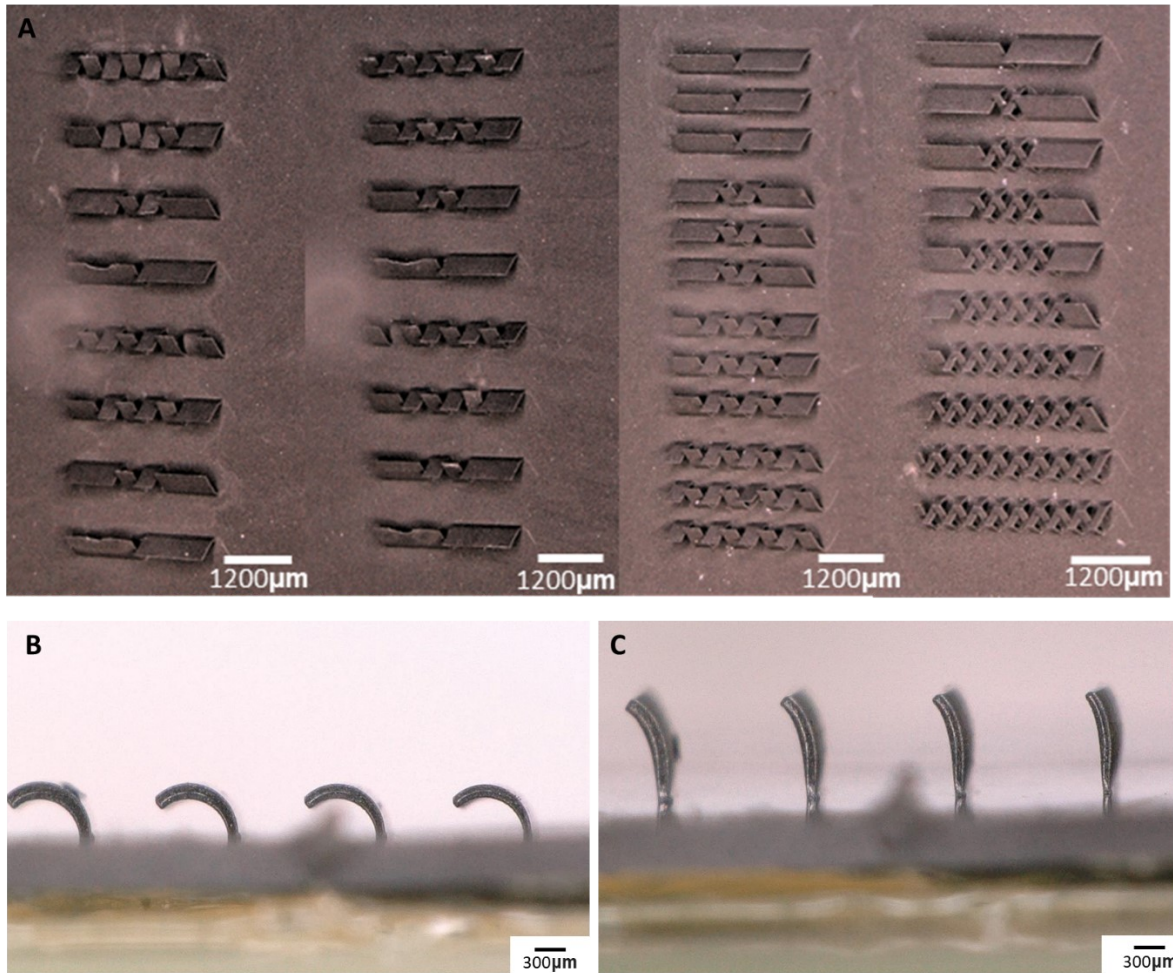


Figure A-8: (A) Various configurations of microwalls and flaps created by the FLAE/molding process. (B) side view of curled microflaps at rest. (C) Curled microflaps actuated under a vertical magnetic field.

Supplementary movie 1 'microwalls.avi': Real-time movie from a side view, showing microwalls being actuated in air.

Supplementary movie 2 'water.mp4': Collection of movie clips showing the changes in water flow when the microwalls were repeatedly turned on and off.

Supplementary movie 3 'glycerol.mp4': Collection of movie clips showing the changes in 87 wt% glycerol flow when the microwalls were repeatedly turned on and off.

Supplementary movie 4 'actuation tracing.avi': A real-time movie showing a 350 μm long and 30 μm microwall with a triangle base actuated with an electromagnetic setup for measurement of tip displacement and tip speed (magnetic flux density 150 mT, see Supplementary Information for more details).

1. Pereira, I. C. F., Wyss, H. M., Pinchuk, L., Beckers, H. J. M. & den Toonder, J. M. J. A model for designing intraocular pressure-regulating glaucoma implants. *PLoS One* **17**, e0273672 (2022).
2. White, F. M. *Viscous Fluid Flow*. (McGraw-Hill, 1991).